

NONTRONITE SPECTRAL REFLECTANCE CHARACTERISTICS WITH IMPLICATIONS FOR MARS SURFACE DETECTION. N. Turenne¹, S. Sidhu¹, D. Applin¹, E. Cloutis¹, S. Mertzman². ¹Centre for Terrestrial and Planetary Exploration, University of Winnipeg, Winnipeg, Manitoba R3B 2E9, Canada. turenne-n@web-mail.uwinnipeg.ca ²Department of Earth and Environment, Franklin and Marshall College, P.O. Box 3003, Lancaster, PA, 17604-3003 USA.

Introduction: Spectral signatures indicative of clay minerals have been observed using the Compact Reconnaissance Imaging Spectrometer for Mars (CRISM) and the Observatoire pour la Mineralogie, l'Eau les Glaces et l'Activite (OMEGA) [1, 2]. Nontronite $[\text{Ca}, \text{Na}, \text{K}]^{0.3}\text{Fe}^{2-3+}(\text{Si}, \text{Al})_4\text{O}_{10}(\text{OH})_2 \cdot n\text{H}_2\text{O}$, an Fe-rich smectite clay has been detected in multiple locations on the Martian surface including north of the Syrtis Major volcanic plateau, Mawrth Vallis and Nili Fossae [1, 2]. The spectral identification of nontronite on Mars has been based on the ~1410, ~2290 and ~2400 nm absorption bands [3].

Nontronite is one of the most abundantly observed Fe^{3+} -smectite clays on Mars [3]. While the regions of phyllosilicate observations are dated to the Noachian [1], the exact formation processes, such as weathering of basaltic materials [4], hydrothermal activity [3] or impact heating [5] are still debated.

The structure of smectite clays consists of tetrahedral-octahedral-tetrahedral (TOT) layers, weakly bonded to other TOT layers by interlayer cations and molecules that balance the negative charge of the TOT layer; this is also where water can be adsorbed [6]. The interlayer also allows expanding or swelling smectites to serve as a site for several organic reactions, even in extreme and inhospitable environments [7]. Lab studies have shown that organic synthesis can occur on the surface or in the interlayer of swelling smectites [7, 8].

Methods: Five nontronite samples (NON101-105) were crushed to <45 μm powders and analyzed with reflectance spectroscopy, X-ray diffraction and X-ray fluorescence and wet chemistry to determine the composition of each sample.

Spectroscopy: Reflectance spectra were acquired using <45 μm powders with an Analytical Spectral Devices LabSpec 4 Hi-Res® spectrophotometer to collect reflectance spectra from 350 to 2500 nm at a viewing geometry of $i=30^\circ$ and $e=0^\circ$. The general mineralogy of the samples was determined using bulk <45 μm powders with a Bruker D8 Advance X-ray diffractometer. Compositional analysis was carried out at Franklin and Marshall College using X-ray fluorescence (XRF) to identify major and selected minor elements and wet chemistry (WC) to determine ferrous iron content.

NON101 was used for a heating experiment and Mars-like surface exposure to better understand its stability field in the context of Mars surface conditions and possible impact-induced heating. Subsamples were

heated to 110°C, 180°C and 300°C for one week each in a CO_2 atmosphere and also subjected to various periods of exposure to a 5 Torr CO_2 atmosphere. Reflectance spectra were acquired after each temperature excursion and before, during, and after the 5 Torr run [9].

Results: Spectrally, Fe^{3+} produces a variety of bands in the shorter wavelength region: ~450 nm, ~650 nm and ~950 nm. Compositionally NON104 contains the most Fe_2O_3 wt.% as seen from Table 1 and exhibited the best-defined Fe^{3+} -associated absorption features below 1000 nm. The spectra exhibit $\text{H}_2\text{O}/\text{OH}$ bands near 1400 and 1900 nm, along with a characteristic metal-OH (Fe^{3+}) band at 2280 nm [10]. A slope decrease is present past 2280 nm, and a weak likely metal-OH absorption band is found at ~2400 nm. (Fig. 1).

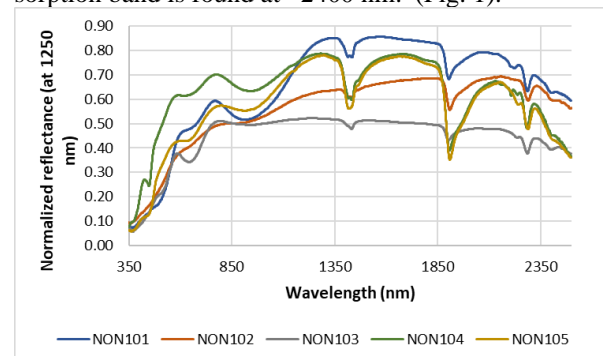


Figure 1. Reflectance spectra for NON101-105 collected using <45 μm powders.

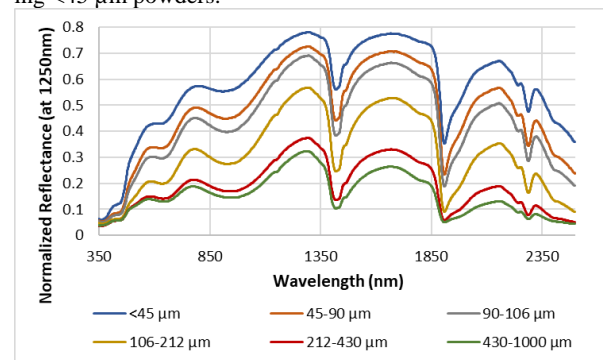


Figure 2. Reflectance spectra for NON105 acquired for different grain sizes.

Grain size: The NON105 spectra exhibit a decrease in intensity with grain size increase, along with widening of the ~1400 and 1900 nm $\text{H}_2\text{O}/\text{OH}$ absorption features (Fig. 2). The 2280 nm band becomes less resolved and decreases in apparent depth with an increase in grain size.

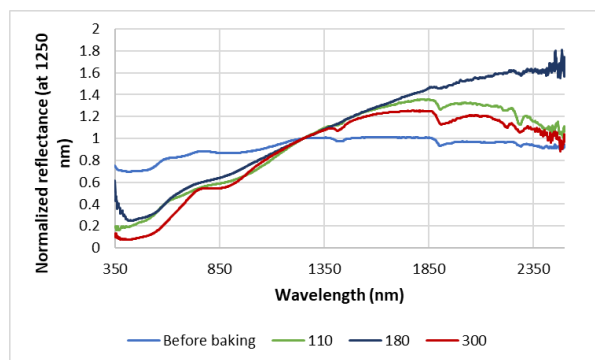


Figure 3. NON101 heating to 110, 180 and 300°C with no sapphire window.

Mars surface exposure effects: Both Mars box exposures of NON101 did not affect the robustness of the distinct and diagnostic 2280 nm band [9]. The MB1 exposure to Mars surface condition resulted in a decrease in the ~950 nm band depth as well as an increase in the spectral slope beyond the ~1400 nm H₂O/OH band, but retained its Fe³⁺-associated feature at 2280 nm, while the MB5 run spectra showed insignificant changes over the course of the experimental run. Upon exposure to 110, 180 and 300°C, NON101 showed spectral slope changes and decreases in depths of the ~1400, ~1900 and 2280 nm bands. Along with the shift in color from a yellowish green to a reddish brown associated with the slope decrease shortward of 1000 nm wavelength. The two Mars-like surface exposure experiments and the (simulated impact-induced) heating did change many spectral properties, but the diagnostic bands in the 1400, 1900, and 2280 nm region were still detectable, therefore nontronite would be deemed spectrally detectable on Mars (Fig. 3).

Table 1. Compositions of NON101-105.

Wt. %	NON101	NON102	NON103	NON104	NON105
SiO ₂	61.40	55.47	56.08	51.98	54.04
Al ₂ O ₃	9.49	9.92	4.89	9.14	8.09
TiO ₂	0.38	0.21	0.56	0.23	0.46
Fe ₂ O ₃	22.08	29.13	34.15	35.20	0.14
FeO	0.79	0.48	0.65	0.17	33.13
(Fe ₂ O ₃)*	(22.96)	(29.66)	(34.87)	(35.39)	(33.29)
MgO	1.07	1.16	0.98	1.10	1.60
CaO	0.10	0.20	1.79	2.18	2.48
Na ₂ O	0.15	0.02	0.52	0.17	0.01
K ₂ O	3.67	2.32	0.06	0.11	0.02
MnO	0.03	0.03	0.01	0.01	0.03
P ₂ O ₅	0.51	0.46	0.09	0.02	0.03
SO ₃			0.06		
TOTAL	99.76	99.45	99.91	100.33	100.05
LOI	8.56	14.46	9.79	21.92	23.11
ppm					
Sr	40	12	112	59	32
Zr	445	117	70	<2	26
V	70	24	220	124	196
Cr	15	<2	68	<2	<2
Ni			13		
Co			<1		
Rb		22		<2	<2
Ba		341		43	49
Source	Mertzman	Mertzman	Mertzman	Mertzman	SCMR
Analysis	XRF/WC	XRF/WC	XRF/WC	XRF/WC	

Composition: The XRD data indicated some impurities in the nontronite samples, while the XRF data indicate compositional differences, which could account for the small shifts in the position of the 2280 nm feature in the nontronite spectra. The largest compositional differences are for SiO₂, and Fe₂O₃. The former can be due to the presence of quartz as indicated by XRD.

Discussion: Nontronite clays are an important mineral to identify on Mars due to its implications for environmental conditions present during formation, subsequent stability, and associations with organic synthesis.

The distinct spectral feature at 2280 nm is characteristic of nontronites and is the spectral band that sets apart nontronite from other phyllosilicate clay minerals such as hisingerite, montmorillonite, saponite, hectorite, and beidellite.

Even with the presence of impurities as indicated by the XRD and XRF data, the 2280 nm absorption band persists, and can be used as a characteristic absorption band for nontronite detection on Mars.

The heating experiment are consistent with previous thermal studies of nontronite; no interlayer water was lost after heated to 300°C. Gavin and Chevrier (2010) [11] detected that heating to temperatures ~400°C caused interlayer water to be lost, and above 700°C the 2200-2300 nm band decreased in intensity and the centre shifted to lower wavelengths [11].

Our results suggest that nontronite is stable under Mars surface conditions and (impact-induced) heating up to 300°C.

Acknowledgments: We wish to thank the Canadian Space Agency (CSA), the Natural Sciences and Engineering Research Council of Canada (NSERC), the Canada Foundation for Innovation (CFI), the Manitoba Research Innovation Fund (MRIF), and the University of Winnipeg for supporting this study.

References: [1] Bibring J.P., et al. (2006) *Science*, 312, 400–404. [2] Ehlmann B.L., et al. (2011) *Nature*, 479, 53–60. [3] Poulet F., et al. (2005) *Nature*, 481, 623–627. [4] Chevrier V., et al. (2007) *Nature*, 448(7149), 60–63. [5] Fairén A.G., et al. (2009) *LPSC*, XV, 1156. [6] Odom I. E. (1984) *Phil. Trans. R. Soc. London*, 311, 391–409. [7] Williams L.B., et al. (2005) *Geology*, 33(11), 913–916. [8] Adams J.M., et al. (1983) *Clays Clay Miner.*, 31(2), 129–136. [9] Cloutis E.A., et al. (2007) *GRL*, 34(20). [10] Bishop J. (2008) *Clay Miner.* 43, 35–54. [11] Gavin P. and Chevrier V. (2010) *Icarus*, 208(2), 721–734.